ELSEVIER

Journal of Power Sources 62 (1996) 155–159

JOURNAL OF POWER SOURCES

High energy and high power density electrochemical capacitors

J.P. Zheng, T.R. Jow

Army Research Laboratory, Electronics and Power Sources Directorate, Fort Monmouth, NJ 07703-5601, USA

Received 26 November 1995; accepted 11 March 1996

Abstract

High energy density electrochemical capacitors were built with a newly discovered electrode material (amorphous $RuO_2 \cdot xH_2O$). Energy densities as high as 96 J/g (26 Wh/kg) were obtained based on the $RuO_2 \cdot xH_2O$ electrode material alone. However, the power density of the capacitor is low. By mixing $RuO_2 \cdot xH_2O$ powders with about 20% weight of carbon black, power densities greater than 10 kW/kg could be achieved at a delivered energy density of about 72 J/g (20 Wh/kg). Capacitance as a function of cycle life was studied for up to 60 000 cycles. The temperature dependence of capacitance and resistance of the capacitor are also reported in this paper.

Keywords: Capacitors; Ruthenium; Energy density

1. Introduction

Power sources that can provide power densities over 1 kW/kg, energy densities over 5 Wh/kg (18 J/g) or 11 Wh/l (39.6 J/cm^3) and unusual cycleability ($>10^5$ cycles) are urgently needed for a number of technologically important systems [1–3]. These systems include acceleration power for electric vehicles, electrical regenerative braking storage for electric drive systems, power assist to hybrid vehicles, starting power for fuel cells, pulse power for mobile telecommunication and other electronic devices that require high power to operate. State-of-the-art dielectric capacitors [4] can provide power densities many times over 1 kW/kg and have very long cycle life ($>10^6$), but they have energy densities less than 3 J/cm^3. State-of-the-art rechargeable batteries [5,6] can provide energy densities over 115 Wh/kg, but have power densities less than 0.2 kW/kg and short cycle life ($<10^4$). Electrochemical (EC) capacitors, commonly called double-layer capacitors, ultra-capacitors, super-capacitors, or capatteries, provide the best opportunity to meet both the power and the energy requirements for the above systems. In addition, when EC capacitors are coupled with batteries, they can reduce the peak power requirement, prolong the lifetime and reduce the energy requirement (or the size) of the battery.

Energy storage mechanisms for EC capacitors include the separation of charge at the interface between a solid electrode and an electrolyte, and/or fast faradaic reactions occurring at or near a solid electrode surface at the appropriate potential [7,8]. The capacitance corresponding to the former mechanism is generally called double-layer capacitance. The capacitance due to the latter mechanism is often called pseudo-capacitance. Recently, it was found that for an amorphous $RuO_2 \cdot xH_2O$ electrode the fast faradaic reaction could occur not only at the surface of the electrode but also in the bulk of the electrode [9,10], the reason is that the proton can easily permeate through the bulk of the amorphous $RuO_2 \cdot xH_2O$. Because the whole bulk of $RuO_2 \cdot xH_2O$ was utilized for energy storage, the energy storage density of $RuO_2 \cdot xH_2O$ is higher than any other capacitor electrode material in aqueous electrolyte by at least a factor of two [7,11,12].

2. Electrode material

Amorphous $RuO_2 \cdot xH_2O$ powders were used as the active electrode material for capacitors. Preparation processes of electrode materials have been described previously [9]. Briefly, the electrode material could be prepared by the sol–gel process. The $RuO_2 \cdot xH_2O$ powders were obtained by annealing precipitate to a temperature above 100 °C. The precipitate was produced by mixing aqueous solutions of $RuCl_3 \cdot xH_2O$ and NaOH to a pH value of about 7.0. The annealing temperature is a very important parameter for determining the charge storage density of the electrode. It was found that at low temperatures, the $RuO_2 \cdot xH_2O$ is an amorphous material. When the annealing temperature was increased, both the amount of powders in the crystalline phase and the crystallite size of these powders were increased. At

PII S0378-7753(96)02424-X

temperature above 300 °C, anhydrous RuO_2 was formed. It was also found that the maximum charge storage density could be obtained from the electrode that was prepared at the temperature which was just below the critical temperature to form the crystalline phase. An average charge storage density as high as 768 C/g was obtained in the potential range of 0–1.0 V versus a standard calomel electrode (SCE) form a cyclic voltammogram of an amorphous $RuO_2 \cdot xH_2O$ prepared at 150 °C. Such high charge storage density is believed to be due to proton permeation into the bulk of amorphous $RuO_2 \cdot xH_2O$, and due to faradaic reactions occurring not only at the surface but also inside the bulk [9,10].

The resistivity of $RuO_2 \cdot xH_2O$ pellets was measured. Pellets were made by pressing $RuO_2 \cdot xH_2O$ powders under a pressure of about 3600 kg/cm^2. It was found that the resistivity of $RuO_2 \cdot xH_2O$ annealed at temperatures of 100–300 °C was on the order of 10^{-3} Ω cm. This value was two orders of magnitude higher than that of a single crystal RuO_2 [13] and was dominated by the contact resistance between particles. However, the resistivity of $RuO_2 \cdot xH_2O$ pellets is about 50 times lower than that of pellets made by carbon black [14]. The specific surface area of $RuO_2 \cdot xH_2O$ powders decreased with increasing the annealing temperature and was from about 90 m^2/g at 25 °C to about 30 m^2/g at 400 °C.

3. Capacitor design

The configuration of the capacitor is the same as that of an Evans double-layer capacitor [15], five cells connected in series sealed in a tantalum container. A small hole (about 1 mm in diameter) was opened on the top of the tantalum container in order to allow gases to escape from the cell stack.

Fig. 1 shows the cross-sectional view of each cell. The electrode material was pre-wetted by back filling 39 wt.% sulfuric acid solution in vacuum. Two identical electrodes were separated by a porous membrane with a thickness of 25 μm. The porous membrane was impregnated with a sulfuric acid solution. The electrode has a diameter of 1.9 cm and a thickness of 50–200 μm. Three capacitors made with different electrodes were investigated, as shown in Table 1. Capacitor A was made with $RuO_2 \cdot xH_2O$ electrodes. Capacitor B was made with composite electrodes comprised of 90 wt.% $RuO_2 \cdot xH_2O$ and 10 wt.% carbon Black Pearls-2000. Capacitor C was made with composite electrodes comprised of 80 wt.% $RuO_2 \cdot xH_2O$ and 20 wt.% carbon Black Pearls-2000. The purpose of adding carbon black to the electrode was to increase the porosity of the electrode and to decrease the ionic resistance of the capacitor. As a result of the added high surface area of carbon black, the amount of electrolyte absorbed by the electrodes was increased as shown in Table 1. For example, if the electrode was made with $RuO_2 \cdot xH_2O$ powders only, the weight ratio between the solid electrode material and the electrolyte absorbed by the electrode was about 65:35. For the composite electrode used in capacitor C, this ratio was reduced to 39:61. It was found that the performance of the capacitor at high current densities was strongly dependent on the porosity of the electrode.

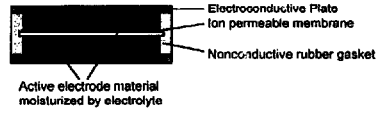

Fig. 1. Cross section of a single cell capacitor.

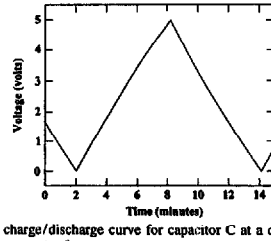

Fig. 2. D.c. charge/discharge curve for capacitor C at a constant current density of 7.0 mA/cm^2. The total weight of 0.22 g of $RuO_2 \cdot xH_2O$ and carbon black was loaded in the capacitor. The average capacitance was calculated from the discharge process.

4. Energy and power densities

Fig. 2 shows the dc charge/discharge characteristics of capacitor C. The average capacitance was calculated by multiplying the current by the time duration of the discharge process and, then dividing by the maximum applied voltage. The total energy stored could be obtained by the following equation [16]

Table 1
Some parameters of electrochemical capacitors made with different electrodes

Devices	Number of cells	Maximum voltage (V)	$RuO_2 \cdot xH_2O$:carbon	c_p [a] (F/g)	Electrode:electrolyte	Mass density (g/cm^3)	Energy density (Wh/kg)
Capacitor A	3	3.0	100:0	768	65:35	2.17	26.7 (17.35)
Capacitor B	5	5.0	90:10	716	57:43		24.7 (14.1)
Capacitor C	5	5.0	80:20	634	39:61	1.787	22.0 (8.6)

[a] The c_p and the energy density were calculated based on the electrode material only. The mass density and the energy density in brackets were calculated based on the electrode material and the electrolyte.

$$E = 1/2CV^2 \quad (1)$$

where C and V are the capacitance and the maximum applied voltage, respectively. Here, it is assumed that the capacitance is independent of the voltage. The energy density of capacitor A was calculated to be 96 J/g based on the $RuO_2 \cdot xH_2O$ material only. This value is more than twice that for capacitors made with RuO_2 thin film electrodes [7,11] and is at least three times higher than that of carbon electrodes with aqueous electrolytes [12]. Energy densities of capacitors made with different electrode materials are listed in Table 1. It can be seen that the energy density decreased when the ratio of carbon in the electrode was increased. From Fig. 2, the energy deliverable efficiency can be easily estimated from the capacity ratio between discharge and charge processes and is over 95%. The capacitance as a function of current density was measured. Results are shown in Fig. 3 for three capacitors made with different electrodes. It can be seen that the capacitance reduced at high current densities. The relationship between capacitance and current density is strongly dependent on the porosity of the electrode. For capacitor A which was made with the low porosity electrode of $RuO_2 \cdot xH_2O$, the capacitance at a current density of 350 mA/cm^2 is only about 40% of that at low current densities. The deliverable energy or energy density of the capacitor will also drop by the same ratio since the energy stored is proportional to the capacitance as shown in Eq. (1). For capacitor C which was made with the highest porosity electrode of three capacitors, the power performance was improved significantly. It can be seen from Fig. 3 that the reduction of the capacitance is less than 10% at a current density of 350 mA/cm^2. The average power density at this current density was calculated to be over 10 kW/kg based on the solid electrode materials only. By introducing the high porous carbon black into the electrode, the power density of the capacitor was enhanced significantly, but the energy density was sacrificed a little. At low current densities, the energy density of capacitor C was calculated to be about 80 J/g (22 Wh/kg) which is about 83% of that obtained from the capacitor A at low current densities. Fig. 9 shows discharge curves of capacitor C at different current densities and demonstrates that the amorphous $RuO_2 \cdot xH_2O$

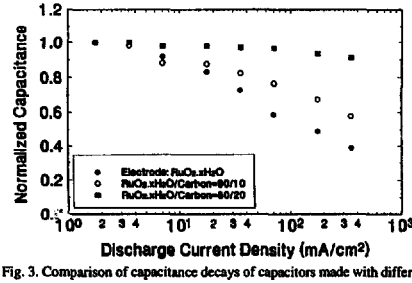

Fig. 3. Comparison of capacitance decays of capacitors made with different electrodes as a function of the discharge current density.

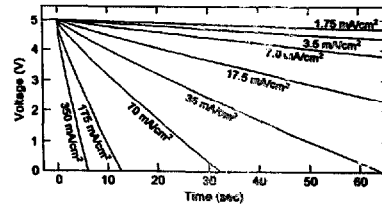

Fig. 4. Discharge behavior for capacitor C at various current densities.

material is capable of high power performance. A small voltage drop at the beginning for high current density cases was due to the internal resistance of the capacitor.

5. A.c. impedance spectra

A.c. resistance and a.c. capacitance spectra were performed on capacitor C. These spectra were recorded in the range from 10 mHz to 10 kHz with a signal amplitude of 5 mV. Figs. 5 and 6 show the equivalent series resistance (*ESR*) and the capacitance spectra at 0, 2.5 and 5.0 V bias. From Fig. 5, it can be seen that the *ESR* is strongly dependent on frequency. From Fig. 6 it can be seen that the capacitance at 5.0 V bias is lower than that at lower biases. This can be easily explained by the result of cyclic voltammetric curves [9,10]. It was found that for potential higher than 0.2 V versus SCE, the current response is insensitive to the potential, but for potentials lower than 0.2 V versus SCE, the current response decreases with the potential. The capacitance of each electrode is proportional to the current response and the capacitance of the capacitor results from two electrodes in series as shown in Fig. 1. At lower biases, the potentials for both electrodes is about 0.5 V versus SCE. The capacitance should be about 1/2 the value of capacitance of each electrode. However, at high biases, the potentials of the positive electrode and the negative electrode were shifted to high and low potentials, respectively. The potential difference should always equals the bias voltage. When the negative electrode has a potential lower than 0.2 V versus SCE, the capacitance of the negative electrode is lower than that of the positive electrode. Therefore, the capacitance is lower than at high bias cases. On the other hand, the value of the capacitance measured at 10 mHz is consistent with that calculated from the voltage drop during the d.c. discharge as shown in Fig. 2.

The leakage current could be calculated from the voltage change as a function of time in a self-discharge curve ($i = C\,dV/dt$), where C is the d.c. capacitance. The leakage current density of the capacitor C was estimated to be about 30 μA/cm^2 at about 4 V bias. The leakage current density is believed to be mainly dependent on the impurity concentration in the electrolyte and the thickness of the porous membrane. By using thick membrane, the leakage current density can be reduced; however, the *ESR* of the capacitor will be increased.

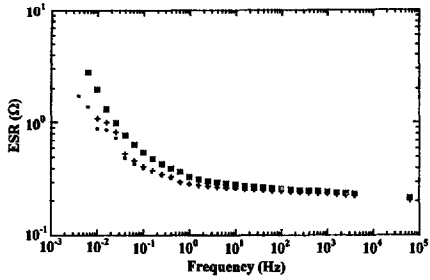

Fig. 5. *ESR* as a function of frequency for capacitor C at (■) 0, (+) 2.5, and (•) 5.0 V biases.

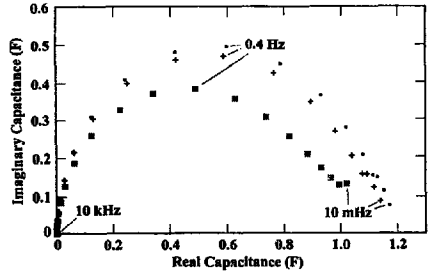

Fig. 6. Complex capacitance plot for capacitor C at (■) 0, (+) 2.5, and (•) 5.0 V biases.

The trade-off between leakage current density and *ESR* can be decided based on different applications. For instance, for high power applications the *ESR* should be low, therefore, a thinner membrane should be used. On the other hand, for low power applications, a thicker membrane should be used in order to reduce the leakage current and to increase the deliverable energy efficiency.

6. Ambient temperature dependence

Many applications need capacitors which are able to perform over a wide temperature range. For EC capacitors, operational temperature is usual limited by the stability of the electrolyte. In this study, we chose 39 wt.% of a sulfuric acid solution (5.26 M) as the electrolyte because of its wider temperature range and lower resistivity at this concentration. Fig. 7 shows d.c. capacitance and *ESR* at a frequency of 1 kHz as a function of the temperature for capacitor A. It can be seen that within the temperature range from −52 to 73 °C, the variation of capacitance is less than 20%. It can also be seen that the resistance increases with decreasing temperature. The result of the resistance dependence is quite reasonable because the resistivity of the sulfuric acid solution increases with decreasing temperature. This result also indicates that the porous membrane wetted by the electrolyte is the main contributor of *ESR* at low temperatures.

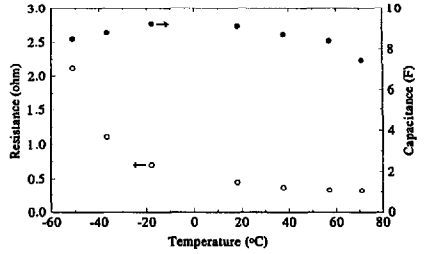

Fig. 7. (●) Capacitance and (○) ESR vs. temperature for capacitor A. The capacitance was measured from the d.c. discharge process and the resistance was measured at 1 kHz.

7. Cycle life test

Unlike batteries, EC capacitors have very long cycle life. Fig. 8 shows the result of the cycle lifetime test for capacitor C. During the test, the current density was 70 mA/cm^2 in a voltage range from 0 to 4 V. Each cycle took less than 40 s. It can be seen that the capacitance decreases about 15% within the first 10 000 cycles. Within 10 000 to 50 000 cycles, the capacitance decays at a much slow rate. After 50 000 cycles, the capacitance decays rapidly again. It can also be seen that the *ESR* increases with cycle number within the first 10 000 cycles, decreases slightly afterwards and then remains constant up to about 50 000 cycles. After 50 000 cycles, the resistance increases again. The decrease in capacitance with cyclic number can have two causes. The first is that the voltage drops during the change of current directions. If a real capacitor is equivalent to an ideal capacitor in series with a resistor (*ESR*), this voltage drop is $2I(ESR)$ where I is the charge and discharge current. It can be clearly seen from Fig. 9 that the voltage drop during the current reversal and the value of *ESR* increases with increasing the cyclic number.

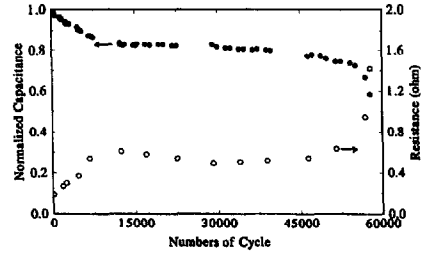

Fig. 8. (●) Capacitance and (○) ESR vs. cycle number for capacitor C. The capacitor was cycled continuously at a current density of 70 mA/cm^2 between 0–4.0 V. The resistance was measured at 1 kHz.

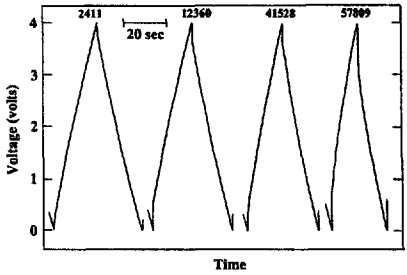

Fig. 9. D.c. charge and discharge behavior at a constant current density of 70 mA/cm² for cycle number of 2411, 12360, 41528 and 57809. The *ESR* at 1 kHz is 0.298, 0.608, 0.655 and 1.422 Ω, respectively.

The second is that the slope (dV/dt) during the charge or discharge processes changes too. It can be seen from Fig. 9 that the slope of dV/dt decreased with increasing cyclic number. The capacitance at a different voltage is defined as $I/(dV/dt)$, therefore the average capacitance decreased with increasing cyclic number.

For a 5-cell capacitor, it was found that if the maximum voltage increased from 4 to 5 V, after several hundred cycles at high current densities the *ESR* was increased by a factor of 100. This observation can be explained by the fact that at high voltage the oxygen gas was generated by the positive electrode of the capacitor. From the cyclic voltammetry measurement, at a potential of 1.2 V versus SCE oxygen gas was generated at the $RuO_2 \cdot xH_2O$ electrode. When the maximum voltage increased, the positive electrode was shifted to a potential close to the potential for oxygen gas evolution. Therefore, oxygen gas was generated in the capacitor. If the gas evolution rate was higher than the rate of gas escaping from the capacitor, the gas would accumulate inside the capacitor to form micro-bubbles. If these bubbles are suspended in the electrolyte or attached on the powder electrode, the resistance of the capacitor will be increased. It should be pointed out that after the capacitor was cycled to a higher voltage for many cycles, the *ESR* increased but the capacitor was not damaged permanently and could be recovered after several days. It should also be pointed that this result does not indicate that a 5-cell capacitor can only operated at a voltage less than 4 V. It was found that the capacitor can still be operational at voltages as high as 5 V at low current densities or even at high current densities as long as it was not charged/discharged continuously for a long period of time. For instance, a capacitor has been charged and discharged for a full voltage range at a current density of 17.5 mA/cm² for over 4000 cycles without significant changes to the resistance and the capacitance. Fig. 4 also demonstrates that a 5-cell capacitor can be operated at the voltage of 5 V and at high current densities.

8. Conclusions

The performance of EC capacitors made with amorphous $RuO_2 \cdot xH_2O$ electrodes and $RuO_2 \cdot xH_2O$/carbon black composite electrodes was demonstrated. A capacitor made with $RuO_2 \cdot xH_2O$ electrodes and H_2SO_4 electrolyte delivered an energy density of 96 J/g (or 26.7 Wh/kg) based on the active hydrous ruthenium oxide only, but the power density was low. However, a capacitor made with composite electrodes could deliver an energy density of over 72 J/g (or 20 Wh/kg) at a power density of above 10 kW/kg based on the weight of $RuO_2 \cdot xH_2O$ and carbon black. It has been demonstrated that capacitors could be safely operated throughout the −52 to 73 °C temperature range. About 60 000 charge/discharge cycles were achieved from a capacitor.

References

[1] A.F. Burke, *Proc. 2nd Int. Seminar Double Layer Capacitors and Similar Energy Storage Devices, Deerfield Beach, FL, USA, 7–9 Dec. 1992.*

[2] S.P. Wolsky and R.S. Wissoker, *The International Technology and Market Study of Electrochemical Capacitors*, Florida Educational Seminars, Boca Raton, FL, 1994.

[3] B.M. Barnett and S.P. Wolsky, *Proc. 4th Int. Seminar Double Layer Capacitors and Similar Energy Storage Devices, Deerfield Beach, FL, USA, 12–14 Dec. 1994.*

[4] T.R. Jow, *Proc. 2nd Int. Seminar Double Layer Capacitors and Similar Energy Storage Devices, Deerfield Beach, FL, USA, 7–9 Dec. 1992.*

[5] S. Sarangapani, P. Lessner, J. Forchione, A. Griffith and A.B. LaConti, *J. Power Sources, 29* (1990) 355.

[6] M.J. Riezenman, *IEEE Spectrum, 51* (May) (1995).

[7] I.D. Raistrick, in J. McHardy and F. Ludwig (eds.), *The Electrochemistry of Semiconductors and Electronics–Processes and Devices*, Noyes, NJ, USA, (1992), p. 297,.

[8] B.E. Conway, *Proc. 2nd Int. Seminar Double Layer Capacitors and Similar Energy Storage Devices, Deerfield Beach, FL, USA, 7–9 Dec. 1992.*

[9] J.P. Zheng and T.R. Jow, *J. Electrochem. Soc., 142* (1995) L6.

[10] J.P. Zheng, P.J. Cygan and T.R. Jow, *J. Electrochem. Soc., 142* (1995) 2699.

[11] I.D. Raistrick and R.T. Sherman, *Proc. Symp. Materials and Processes for Energy Conversion and Storage*, Proc. Vol. 87, The Electrochemical Society, Pennington, NJ, USA, 1987, p. 12.

[12] E. Black, *Proc. 2nd Int. Seminar Double Layer Capacitors and Similar Energy Storage Devices, Deerfield Beach, FL, USA, 7–9 Dec. 1992.*

[13] S. Trasatti and G. Lodi, in S. Trasatti, *Electrodes of Conductive Metallic Oxides — Part A*, Elsevier, New York, 1980, p. 301.

[14] T. Saito, Y. Kibi, M. Kurata, J. Tabuchi and A. Ochi, *Proc. 4th Int. Seminar Double Layer Capacitors and Similar Energy Storage Devices, Deerfield Beach, FL, USA, 12–14 Dec. 1994.*

[15] *The Evans Capattery*, Evans, East Providence, RI, USA.

[16] L.C. Shen and J.A. Kong, *Applied Electromagnetism*, PWS Engineering, Boston, MA, USA, 2nd. edn., 1987, p.322.